JACS
JOURNAL OF THE AMERICAN CHEMICAL SOCIETY
pubs.acs.org/JACS

Article

Direct Visualization of Segment-Like Dynamics in Isolated Polymer Chains on Solid Surfaces

Shuji Morita, Yuma Morimitsu,* Shiho Tanizaki, Tomohiro Kubo, Satoru Yamamoto, Kotaro Satoh,* and Keiji Tanaka*

Cite This: https://doi.org/10.1021/jacs.5c23137

Read Online

ACCESS | Metrics & More | Article Recommendations | Supporting Information

ABSTRACT: The performance of polymer-based composites, coatings, and adhesives is critically governed by the dynamics of chains at solid interfaces, yet their molecular principles remain unresolved. Here, we use time-resolved atomic force microscopy to directly map segment-level relaxation dynamics in isolated polystyrene chains on atomically flat substrates. We uncover pronounced spatial heterogeneity, with some segments accelerating with temperature while others slowing down, a counterintuitive behavior arising from transient adsorption. These dynamics propagate into neighboring chains through interfacial coupling and extend the influence of adsorption beyond direct contacts. Molecular dynamics simulations corroborate the coexistence of thermally activated and adsorption-driven slowing processes, and experiments on catechol-functionalized chains demonstrate generality and relevance to adhesion on metal oxides. Our results establish a real-space framework for linking interfacial structure and chain dynamics. They also reveal isolated chains on solids as nonequilibrium systems, offering a paradigm for molecular-level design of adhesion and interfacial toughness.

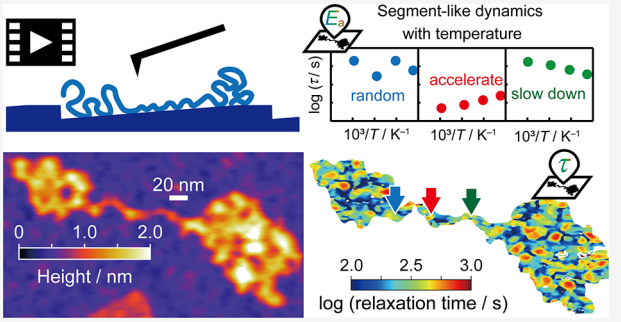

INTRODUCTION

In polymer-based systems used in electronics, energy storage, and structural reinforcement, polymer chains often interact intimately with solid surfaces, and their conformational and dynamic behaviors diverge markedly from those in the bulk.[1−3] At these interfaces, nanoscopic adsorption layers are formed,[4−6] defined by restricted mobility, altered packing, and anisotropic responses. Although only a few nanometers thick, such layers disproportionately control macroscopic properties including adhesion strength, fracture toughness, and dielectric performance.[7−9]

Despite extensive efforts, the molecular principles governing chain dynamics at solid interfaces remain elusive. Most prior studies have relied on ensemble-averaged techniques that obscure spatial and temporal heterogeneity. Neutron reflectometry[10,11] and spectroscopic methods[12,13] have demonstrated slowed segmental mobility near solid interfaces, yet cannot resolve localized relaxation. Molecular simulations predict transient adsorption, cooperative pinning, and desorption[14,15] although direct real-space validation is lacking. In particular, the temperature dependence of segment-level motion under interfacial constraints is unsettled, with conflicting reports of both enhanced and suppressed dynamics.[16−19]

The cooperative nature of interfacial interactions is a critical, yet often overlooked, aspect. While individual monomer-surface contacts are weak ($\sim k_BT$, k_B is the Boltzmann constant and T is the temperature),[20] multiple contacts can kinetically trap segments.[21−23] The restricted dynamics between contact points can further propagate to adjacent chains via pseudoentanglements, extending dynamical suppression beyond the interface.[24−26] Capturing such cooperative, spatiotemporally resolved behaviors requires segment-level resolution.

To directly probe these effects, we employed high-resolution time-resolved atomic force microscopy (AFM)[27] to visualize thermally activated motion of isolated polymer chains adsorbed on atomically flat silicon (Si(111), hereafter Si)[28] and alumina (Al_2O_3) surfaces. To establish fundamental principles, we first used polystyrene (PS) (Figure 1a), a simple and well-characterized model polymer, which isolates the intrinsic features of interfacial chain dynamics while avoiding chemical or architectural complexities.[29] To extend these insights toward application-relevant systems, we then examined PS chains functionalized with catechol groups (Figure 1a), a motif inspired by mussel adhesion,[30] and investigated their

Received: December 25, 2025
Revised: February 17, 2026
Accepted: February 23, 2026

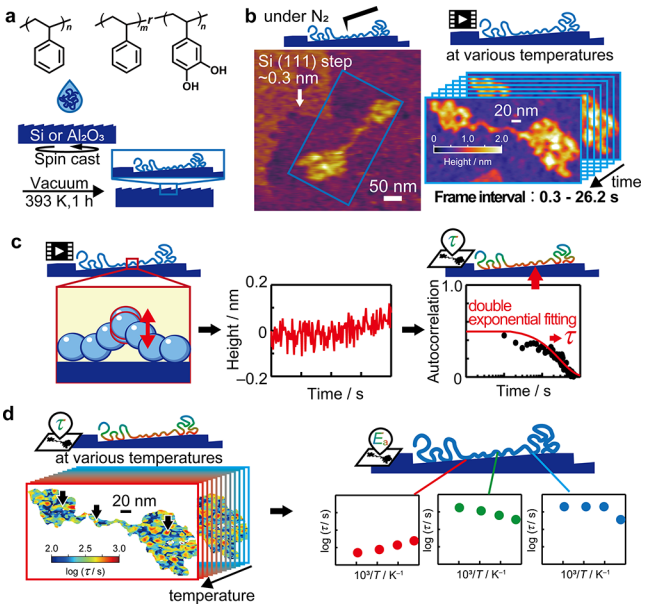

Figure 1. Overview of the workflow for visualizing segment-like dynamics in isolated polymer chains at solid interfaces. (a) Chemical structures of polystyrene and poly(styrene-*random*-vinyl catechol) and schematic illustration of sample preparation by spin-casting dilute polymer solutions onto Si or Al_2O_3 substrates and thermal annealing for 1 h at 393 K under vacuum. (b) AFM measurements for isolated polymer chains on atomically flat substrates under a nitrogen atmosphere. After locating chains by wide-area scanning, higher-magnification imaging was performed, and time-lapse imaging was conducted with frame intervals of 0.3−26.2 s. (c) Mapping of relaxation time (τ) extracted from height fluctuations by fitting the corresponding autocorrelation functions with a double-exponential model. (d) Temperature-series analysis at each position within isolated chains, obtained from the temperature dependent τ maps.

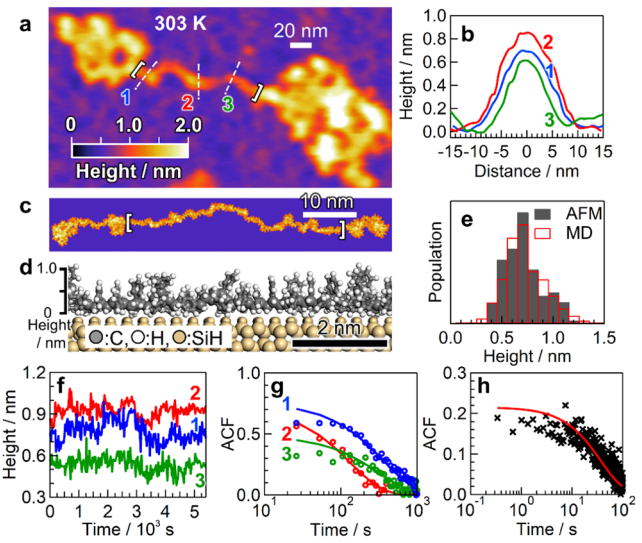

Figure 2. Real-space visualization of dynamics in isolated PS chains on Si. (a) AFM image acquired at 303 K on a sample prepared by spin-casting a highly dilute chloroform solution onto Si, followed by vacuum annealing at 393 K for 1 h. (b) Height profiles along lines 1, 2, and 3 are shown in panel (a). (c) Height map and (d) side view from all-atom MD simulations of an isolated PS chain on Si surface. The height scale in panel (c) matches that in panel (a). (e) Height distributions obtained from AFM measurements (white-bracketed region in panel (a)) and MD simulations (white-bracketed region in panel (c)). (f) Time evolution of chain height at the positions marked in panel (a), measured at 303 K with a frame interval of 26.2 s with a scan size of 400 × 200 nm (1024 × 512 pixels). (g) ACFs of height fluctuations at the same positions corresponding to the data in panel (f). (h) ACF measured at 303 K using video-rate AFM with a frame interval of 0.34 s with a scan size of 400 × 200 nm (512 × 120 pixels).

behavior on Al_2O_3 substrates. Catechol-based functionalities are actively explored in the development of next-generation adhesives for metallic surfaces such as aluminum, a key material in automotive engineering.[31] Tracking subnanometer height fluctuations with subsecond resolution (Figure 1b), we mapped relaxation times at pixel dimensions comparable to the segment length (Figure 1c). Temperature-series analysis revealed both acceleration and counterintuitive slowing of dynamics with increasing temperature (Figure 1d), defying classical expectations and highlighting adsorption-mediated confinement. These interfacial dynamics are neither predicted by bulk activation models nor captured in traditional viscoelastic measurements.

Our findings provide direct evidence of segment-level confinement and establish a generalizable framework for mapping structure−dynamics relationships at the chain level. This approach reveals how local interfacial interactions shape collective relaxation and offers a paradigm for molecular-level design of adhesion and interfacial toughness. Together, these insights have broad implications for polymer-based technologies.

■ RESULTS AND DISCUSSION

Direct Imaging of Isolated PS Chains

Isolated PS chains were deposited on atomically flat Si step-edge substrates via spin-casting from a dilute chloroform solution, followed by vacuum annealing at 393 K for 1 h (Figure 1a). Figure 2a shows the AFM image acquired at 303 K. The observed morphology was typical (Figure S1), consisting of a chain-like portion with globular features at both ends. All AFM measurements were conducted under a nitrogen atmosphere in tapping mode, within the attractive tip−sample interaction regime that minimizes mechanical perturbation to the chains,[32] unless otherwise noted. We confirmed that imaging was performed in the least invasive region of the attractive regime, where no displacement of the polymer segments was induced. In contrast, entering the repulsive regime altered the observed features and compromised dynamic reproducibility.

The height profiles extracted from three cross-sectional positions (Figure 2b; lines correspond to those in Figure 2a) revealed height variations of approximately 0.7, 0.9, and 0.6 nm. The apparent lateral width of the chain was approximately 20 nm. After the deconvolution of the tip-broadening effect, the actual width was estimated to be ∼1 nm (Figure S2).

Molecular dynamics (MD) simulations of a PS chain on a Si surface following thermal annealing showed that the polymer backbone was parallel to the surface, with the phenyl rings predominantly oriented flat against the substrate and occasionally tilted along the surface normal (Figure 2c and d; Figure S3). The simulated structure also displayed globular end features that were qualitatively consistent with AFM observations.

The height distributions obtained from the AFM and MD data (Figure 2e) were in close agreement, and similar consistency was observed in the width distributions (Figure

https://doi.org/10.1021/jacs.5c23137
J. Am. Chem. Soc. XXXX, XXX, XXX−XXX

S4). The volume estimation of the observed structure (Figure S5), in combination with these structural features, is consistent with the presence of two PS chains.

Time-Resolved Dynamics in Isolated Chains

To investigate the localized chain dynamics in an isolated PS chain, we continuously monitored the chain morphology for 90 min at 303 K using time-lapse AFM imaging with a frame interval of 26.2 s. The lateral drift was corrected via postprocessing.[33−35] Figure 2f shows the temporal evolution of the chain height at three labeled positions (1, 2, and 3) each exhibiting spontaneous fluctuations (see also Movie S1). The amplitudes were negligible on the bare substrate but finite over polymer chains, indicating that the observed fluctuations reflect genuine chain motion rather than instrumental artifacts (Figure S6). As shown in Movie S1, the in-plane fluctuations of the targeted segments were also detectable. However, these lateral fluctuations were constrained by adsorption points, and the degree of restriction depended on the segment's height above the substrate. Therefore, we focus on the vertical height fluctuations.

To quantify these motions, we computed the autocorrelation function (ACF) of the height fluctuations at each position (see Methods in Supporting Information for details). The ACFs exhibited an abrupt drop from lag 0 to lag 1 (Figure S7), followed by a slower decay (Figure 2g). The initial drop reflects motion occurring faster than the imaging rate, whereas the gradual decay corresponds to longer relaxation processes.

These ACFs were fitted using a double-exponential model to obtain the two relaxation times. The slower component, denoted τ_{slow}, ranged from 131 ± 10 to 363 ± 13 s across the positions, where ± indicates the standard deviation, indicating a spatial variation in chain mobility. These fluctuations are "segment-like" in nature because they refer to localized motions on the nanometer scale, although they may differ from the segmental dynamics classically defined in polymer physics, which typically involve cooperative motion among surrounding segments.

To assess the faster component, we performed video-rate AFM imaging with a frame interval of 0.34 s. This revealed a fast relaxation process with a characteristic time (τ_{fast}) of 37 ± 2 s. The average τ_{fast} was 40 ± 10 s and showed little positional dependence (Figure 2h and Figure S8e). Imaging the same region with a longer frame interval (25.6 s) revealed slower dynamics consistent with τ_{slow}, confirming the coexistence of fast and slow processes (Figure S8c). Synthetic time-series data generated using a first-order autoregressive [AR(1)] model (Figure S9) demonstrated that short frame intervals preferentially capture faster modes, whereas longer intervals emphasize slower relaxation.

A transient drop in ACF from lag 0 to lag 1 was consistently observed even at a frame interval of 0.34 s, attributable to instrumental noise intrinsic to the AFM setup. However, measurements with frame intervals of 12.8 and 25.6 s confirmed that the derived relaxation times were independent of frame intervals, although the magnitude of the initial drop varied with noise levels (Figure S8c).

Using a sufficiently low tapping force was critical for observing chain dynamics, which was achieved here by measurements under attractive interaction conditions using a minimal tapping force. Negative control experiments under repulsive conditions (tapping force 0.08 nN, smaller than in typical AFM conditions) revealed that tip−sample interactions influence the observed dynamics. Under these conditions, the ACF at lag 1 [ACF(1)] was near zero (Figure S8d), indicating that height signals were dominated by random perturbations arising from nonconstant tip−sample forces rather than intrinsic polymer motion, consistent with the fact that ACF for random white noise drops from 1 to 0 between lag 0 and lag 1. In contrast, all AFM data presented in the main text were obtained under attractive interaction conditions with minimal tapping force. These consistently exhibited finite ACF(1), indicating negligible influence by tip−sample interaction (Figure S10), demonstrating successful detection of time-correlated height fluctuations that reflect segment-like motion within individual chains. Owing to the finite observation window, some pixels exhibited corrupted ACF profiles (ACF(1) near zero or deviating from a double-exponential). Such pixels were excluded from τ mapping and temperature-dependent analyses.

In addition, only polymer chains adsorbed on the flat Si(111) terraces were analyzed. Segments located at or near step edges, formed during etching due to the wafer's finite miscut angle, were excluded. Thus, atomic steps do not contribute to the segment-like dynamics discussed here. Although not directly involved in the observed dynamics, the step edges provide useful internal references that enhance measurement reliability, enabling accurate height calibration, thermal drift correction, estimation of the effective AFM tip radius, and verification of low noise levels in time-resolved AFM observations.

Mechanistic Origin of Dual Relaxation Times

What are the molecular origins of these two relaxation processes observed at 303 K, namely those associated with time scales of $\tau_{fast} \sim 40$ s and τ_{slow} at hundreds of seconds? In bulk PS, side chain motions such as phenyl ring rotations occur on the time scale of 10^{-7} s at room temperature[36] and are generally insensitive to the environment. Therefore, the observed fluctuations cannot be attributed to side-chain dynamics.

Two distinct backbone relaxation modes have been identified in bulk systems: local crankshaft-like twisting and cooperative segmental motion involving multiple repeat units.[37,38] The former occurs independently of the presence or motion of the surrounding segments, whereas the latter requires cooperative movement of neighboring segments. Although it is difficult to definitively assign the observed height fluctuations to a specific molecular motion, the differences in relaxation times suggest varying degrees of collective motion. We tentatively assigned τ_{fast} to localized motions and τ_{slow} to more cooperative segment-like motions within the same chain. To distinguish these interfacial dynamics from conventional bulk behavior, we refer to them as "segment-like" motions, reflecting their modulation by surface interactions, particularly chain adsorption.

Notably, the observed dynamics are distinct from the bulk segmental relaxation, which is frozen at 303 K below the glass transition temperature. However, in isolated chains, looped segments that are not adsorbed onto the substrate may retain mobility. Owing to the lack of surrounding constraints, these unadsorbed loops can exhibit relatively large-scale motion independent of the glassy state. Therefore, we propose that τ_{slow} can reflect the real-space dynamics of such mobile loop segments.

https://doi.org/10.1021/jacs.5c23137
J. Am. Chem. Soc. XXXX, XXX, XXX−XXX

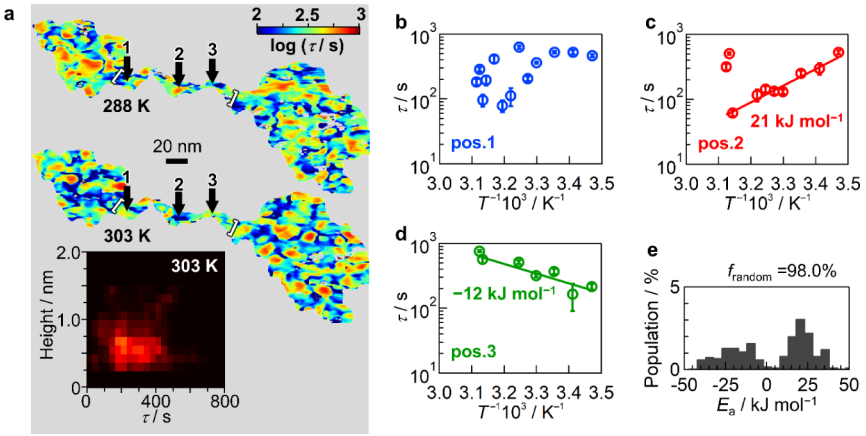

Figure 3. Temperature-dependent segment-like dynamics of isolated PS chains on Si. (a) Heatmaps of τ extracted from ACFs on a pixel-by-pixel basis at 288 and 303 K. (Inset) Two-dimensional histogram of the string-like regions (white-bracketed region in panel (a)), showing the relationship between relaxation time (X-axis) and chain height (Y-axis) at 303 K. (b to d) Arrhenius plots of τ at positions (b) 1, (c) 2, and (d) 3, as marked in Figure 2a. (e) One-dimensional histogram of activation energy (E_a) for PS chains of string-like regions (white-bracketed region in panel (a)). The value of f_{random} is also indicated.

Temperature Effects on Chain Dynamics

To examine the spatial distribution of relaxation times, τ_{slow} was extracted from the ACFs on a pixel-by-pixel basis. Because the subsequent analysis focuses solely on τ_{slow}, it will be simply denoted as τ. Figure 3a shows the heatmaps of τ at 288 and 303 K. The spatial variation reflects differences in local chain conformation at the solid surface.

Notably, fully adsorbed (i.e., immobile) segments do not contribute to height fluctuations and may therefore be buried within the surrounding mobile regions. By comparing the τ maps at different temperatures ranging from 288 to 321 K, both acceleration and deceleration of relaxation were observed at different locations. Figure 3b–d shows the Arrhenius plots of τ at positions 1, 2, and 3. At temperatures above 321 K, the lateral motion transitioned from mere fluctuations to pronounced morphological changes, precluding the analysis of segment-like dynamics under these conditions.

At position 1, τ deviates from the Arrhenius behavior. This deviation likely reflects a complex combination of factors similar to those described in the following paragraph. That is, while some thermally activated processes may be present, the overall temperature dependence is influenced by competing effects such as local interactions with the substrate. Figure 3e quantifies the fraction of such non-Arrhenius segments (f_{random}) within the string-like region, as shown in Figure 2a. The high frandom value (98.0%) indicates that most segments were in nonequilibrium states.

In contrast, the τ value at position 2 shows clear Arrhenius-type behavior, namely decreasing at higher temperatures. This suggests that the dynamics at this site are thermally activated. The local conformation appears relatively stable over the examined temperature range, corresponding to a quasi-equilibrium state. Unexpectedly, a negative Arrhenius-type dependence is observed at position 3, where τ increases with temperature. This counterintuitive behavior implies that the dynamics at this location become slow at increased temperatures, potentially reflecting the complex local interactions that resist thermal activation, such as adsorption onto the substrate.

Insights into Dynamic Heterogeneity from MD Simulations

To elucidate the molecular origins of the three types of temperature dependence observed in the dynamics of isolated PS segments, namely random, positive Arrhenius-type, and negative Arrhenius-type behaviors, we performed all-atom MD simulations of a PS chain adsorbed on a Si substrate. The mean square displacement (MSD) of each backbone segment was calculated at various temperatures.

Consistent with experimental observations (Figure S11), many segments in the MD simulations exhibited irregular or random temperature dependences. The other segments became increasingly mobile with increasing temperature (Figure S12), corresponding to positive Arrhenius-type behavior. In contrast, some segments showed decreasing mobility with increasing temperature, indicative of negative Arrhenius-type behavior (Figure S13). Thus, the MD results establish mechanistic consistency with the three types of temperature dependence observed in isolated PS segments by AFM and demonstrate that these chain dynamics intrinsically arise from chain-level processes, even though the simulation time scale (100 ns) is many orders of magnitude shorter than the experimental time scale (10–1000 s).

Figure S13a shows the snapshots of a representative segment protruding from the substrate. As the temperature increased, the height gradually decreased, indicating progressive adsorption. This trend is corroborated by the MSD data in Figure S13b, indicating a decline in mobility. This behavior likely results from cooperative adsorption involving neighboring segments,[25] which suppresses local motion. Figure S13c further supports this mechanism, showing that the peak of the local carbon density profile shifts toward the substrate with increasing temperature.

Figure 3e shows the distribution of the activation energy (E_a), which represents the energy barrier of the observed dynamic processes. The positive E_a values were broadly distributed, with a peak at approximately 20 kJ mol^{-1}. This value is significantly lower than that of segmental motion in bulk PS (360–880 kJ mol^{-1}).[37] A key factor underlying the reduced activation energy is the small number of segments involved in cooperative motion. In bulk polymers, segmental

https://doi.org/10.1021/jacs.5c23137
J. Am. Chem. Soc. XXXX, XXX, XXX−XXX

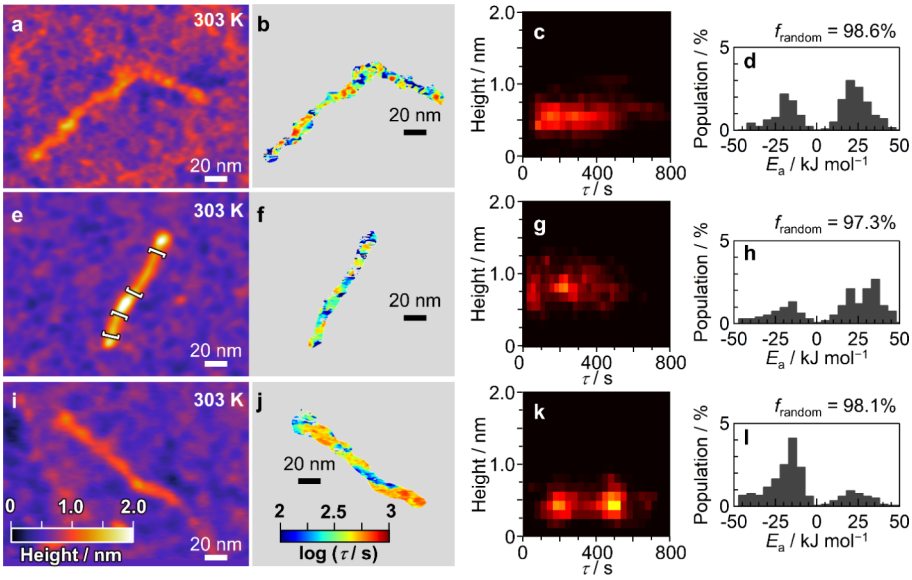

Figure 4. Influence of interfacial interactions on segment-like dynamics in isolated chains across different polymer−substrate combinations. (a−d) PS on Al_2O_3, (e−h) P(St-*r*-VCa)12 on Si, and (i−l) P(St-*r*-VCa)12 on Al_2O_3. (a, e, and i) AFM images acquired at 303 K of isolated chains annealed at 393 K for 1 h under vacuum. (b, f, and j) Heatmaps of τ extracted from ACFs on a pixel-by-pixel basis at 303 K. (c, g, and k) Two-dimensional histograms showing the relationship between τ (*X*-axis) and chain height (*Y*-axis) at 303 K. (d, h, and l) Histograms of E_a. The value of f_{random} is also indicated at the top. The histograms for P(St-*r*-VCa)12 on Si (panels g and h) were generated using data extracted from the string-like region (white-bracketed area in panel e).

dynamics are inherently collective and are commonly described within the Adam−Gibbs framework,[39] leading to large activation energies due to the involvement of many surrounding segments. In contrast, in the present system, the cooperative unit is markedly reduced, potentially involving only a few adjacent segments. Reductions in activation energy have also been reported for polymer surfaces (∼200 kJ mol^{-1}),[40] where the absence of neighboring segments on one side lowers the barrier compared to the bulk. In the present system, the moving segments are surrounded by a low-density gaseous environment rather than other polymer chains, reducing frictional constraints even more. Taken together, these factors rationalize an activation energy on the order of 20 kJ mol^{-1}. These results indicate that neighboring segments play a decisive role in amplifying the activation barrier. Side and bottom neighbors increase E_a by approximately 10-fold, and full three-dimensional confinement can increase it by 20−40 times.

Negative E_a values were also observed, with peaks at approximately −10 and −20 kJ mol^{-1}. The adsorption enthalpy of a single segment is known to be on the order of k_BT,[20] which is consistent with these values. The MD results indicate that the effective energy barrier in these cases arises from the conformational rearrangement of the surrounding chains required for adsorption, which aligns with the observed E_a values. The component near −10 kJ mol^{-1} is likely associated with the crankshaft-type motion of the PS backbone.[41]

Adsorption-Driven Modulation of Chain Dynamics

To evaluate the influence of interfacial interactions on the segment-like dynamics in isolated chains, we examined a random copolymer, poly(styrene-*random*-vinyl catechol) with 12 mol % vinyl catechol units [P(St-*r*-VCa)12],[42] on two substrates of Si and Al_2O_3 prepared by atomic layer deposition. For comparison, PS was also tested on Al_2O_3. The annealing conditions matched those used for PS on Si.

String-like features were observed in all samples. The τ heatmaps revealed spatial heterogeneity similar to that observed for PS on Si. Two-dimensional histograms of τ versus height (Figure 4c, g, and k; cf. inset of Figure 3a) show that the τ distributions were altered by both the introduction of VCa units and the choice of substrate.

For PS, the τ distribution was broad for up to 500 s, regardless of the substrate. In contrast, P(St-*r*-VCa)12 showed bimodal τ distributions. On Si, the peaks appeared at ∼75 and ∼225 s, whereas on Al_2O_3, they shifted to ∼200 and ∼500 s. Given the low VCa content (12%), these dynamic features likely reflect the motion of the PS segments influenced by nearby VCa units. This behavior reflects the strong affinity of catechol groups for Al_2O_3 surfaces,[30,43] which enhances local adsorption and restricts the mobility of both the catechol and neighboring styrene segments, thereby shifting the τ distribution toward longer times.

Contrary to expectations, the primary peak of positive E_a remained at ∼20 kJ mol^{-1} for all the samples (Figures 3e, 4d, h, and l). This result is reasonable because most of the observed motions were attributed to the PS segments. Highly immobilized VCa segments, which are strongly bound to the surface, may not contribute to height fluctuations and thus remain undetected. Interestingly, the P(St-*r*-VCa)12 on Si exhibited an additional E_a peak at ∼30 kJ mol^{-1}. This sample also exhibits a relatively high chain height (Figure 4g) than those of other combinations (Figure 4c and k), indicating more frequent loop formation. The increased local density in these regions may constrain the motion and promote cooperative relaxation, thereby increasing the observed activation energies.

When we changed the substrate from Si to Al_2O_3, the peak position of the negative E_a for PS was the same, that is, −20 kJ mol^{-1}. However, for P(St-*r*-VCa)12, the peak shifts to −15 kJ

https://doi.org/10.1021/jacs.5c23137
J. Am. Chem. Soc. XXXX, XXX, XXX−XXX

mol^{-1}. This trend implies that stronger interfacial interactions between the VCa units facilitate segmental adsorption by promoting the rearrangement of the surrounding chains. The larger relative population of segments exhibiting a negative E_a on Al_2O_3 further supports this hypothesis.

To assess the adsorption-induced rearrangements, we thermally cycled P(St-*r*-VCa)12 on Al_2O_3 to 323 K and then conducted measurements at 303 K. As shown in Figure S14, τ increased in certain regions, and the population near 600 s was enhanced in the 2D histogram, indicating that heating-induced conformational changes favored stronger interactions with the substrate. Notably, Al_2O_3 is a technologically important substrate for multimaterial integration strategies for next-generation mobility platforms. Thus, the ability to alter local chain dynamics through interfacial chemistry represents a powerful molecular-level tuning mechanism. This finding shows that interfacial chemistry can directly modify local relaxation landscapes and offers a molecular-scale means of adjusting polymer dynamics at solid surfaces. Such control is not achievable through bulk measurements.

Confined Dynamics in Globular Regions

Finally, we investigated how the surrounding segments affect the segment-like dynamics by analyzing the behavior within globular regions. Figure 5b–d shows the Arrhenius plots of τ at

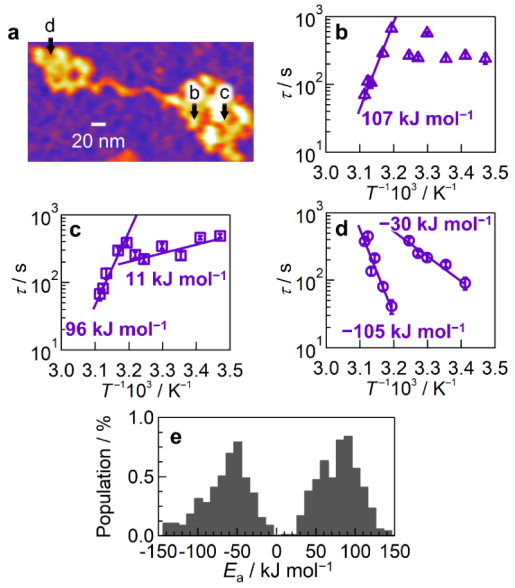

Figure 5. Thermally activated segment-like motion in globular regions of PS chains adsorbed on Si. (a) AFM image acquired at 303 K. (b–d) Arrhenius plots of τ at the positions marked by arrows in panel (a), showing temperature-dependent relaxation behavior at different locations. (e) One-dimensional histogram of E_a extracted from the globular region at temperatures ranging from 313 to 321 K.

the locations indicated by arrows in Figure 5a. At position b, τ exhibited random behavior up to approximately 313 K; however, a transition to positive Arrhenius-type behavior emerged at higher temperatures, with an E_a of 107 kJ mol^{-1}. At positions c and d, both positive and negative Arrhenius-type responses were observed at lower temperatures, and the E_a values were comparable to those seen in the string-like regions. At higher temperatures, these positions showed distinct Arrhenius-type behavior, with E_a values of 96 and −105 kJ mol^{-1}, respectively. This trend suggests that the segment-like motion at elevated temperatures becomes increasingly cooperative and involves neighboring segments. The increased effective mass of the moving units leads to a higher E_a. Notably, the number of cooperatively moving segments remains limited, because lateral motion is not dominant under these conditions.

A histogram of E_a (Figure 5e) revealed peaks at approximately 60, 90, and −50 kJ mol^{-1}, respectively. These values are comparable to those reported for various dynamic processes in bulk systems, including local twisting motion,[37] dewetting phenomena,[44] physical aging,[45] and slow Arrhenius processes.[46] This alignment suggests that confinement-induced cooperative rearrangements in isolated chains resemble universal slow processes that are known in polymer physics.

The observed dynamics differ fundamentally from side-group β-relaxation in both time scales and physical character. The relaxation times are substantially longer than those typically associated with β-relaxation, and the dynamics exhibit pronounced environmental dependence, including the coexistence of two relaxation modes at a single location and a marked increase in activation energy within globular regions. These characteristics indicate that the motion involves main-chain segments rather than localized side group rotations. Therefore, a direct comparison of activation energies with β-relaxation is not appropriate.

Concluding Remarks

Understanding the behavior of isolated polymer chains on solid surfaces is a longstanding challenge in polymer science, with broad implications for adhesion, coating, and composite performance. In this study, we directly visualized the thermally activated motion of isolated chains of PS and P(St-*r*-VCa)12 on atomically flat Si and Al_2O_3 substrates using real-space AFM.

By quantifying subnanometer-scale height fluctuations, we extracted the relaxation dynamics at the segmental level and revealed spatially heterogeneous temperature-dependent behaviors strongly influenced by interfacial interactions. The segment-like motion not only accelerated, but also decelerated with increasing temperature, with the latter reflecting spontaneous adsorption events. The emergence of negative Arrhenius-type behavior in confined regions demonstrates that adsorption competes with thermal activation and can produce unconventional slowing upon heating. The distribution of activation energies further supports this interpretation, linking the observed behavior to known bulk phenomena, such as twisting motions, dewetting, and physical aging.

Although PS was selected as a model system due to its well-established hierarchical dynamics, similar adsorption–desorption events have been visualized for isolated poly(methyl methacrylate) (PMMA) chains[47] and double-stranded DNA on solid substrates,[25] indicating that such interfacial dynamics are not unique to PS. Moreover, by introducing substrate-binding motifs such as catechol groups into the polymer chain, as exemplified by P(St-*r*-VCa)12, we demonstrated that the local chain dynamics at the substrate interface can be modulated, thereby enabling control over interfacial adhesion. This molecular-level tunability indicates that interfacial mechanics can be engineered from the bottom up.

With this methodological framework, the present approach can be extended to polymers with different chemical structures and interfacial affinities. The results indicate that adsorption-modulated segmental dynamics may represent a general

https://doi.org/10.1021/jacs.5c23137
J. Am. Chem. Soc. XXXX, XXX, XXX−XXX

characteristic of polymer-surface systems rather than a phenomenon specific to PS.

Our approach offers a general framework for linking the structures, dynamics, and functions of confined polymer systems, with important implications for adhesives, coatings, and composite interfaces. Taken together, our findings show that isolated polymers on solid substrates exhibit thermally driven dynamics fundamentally distinct from bulk equilibrium behavior due to adsorption-mediated cooperativity and confinement. Recognizing this behavior opens a new conceptual space for understanding and controlling molecular processes at interfaces and provides a foundation for rational molecular design of interfacial materials.

■ ASSOCIATED CONTENT

Supporting Information

The Supporting Information is available free of charge at https://pubs.acs.org/doi/10.1021/jacs.5c23137.

Time-lapse AFM imaging of PS chains on Si at 303 K, acquired at a frame interval of 26.2 s; scale bar is 50 nm (MP4)

Description of materials; sample preparation; experimental details for AFM, MD simulation, and data modeling; results for AFM, data modeling analysis, differential scanning calorimetry, thermogravimetric analysis, proton nuclear magnetic resonance spectra, and size-exclusion chromatography; detailed analysis for AFM and MD (PDF)

■ AUTHOR INFORMATION

Corresponding Authors

Yuma Morimitsu − *Department of Applied Chemistry, Kyushu University, Fukuoka 819-0395, Japan;* orcid.org/0000-0001-7303-0006; Email: y-morimitsu@cstf.kyushu-u.ac.jp

Kotaro Satoh − *Department of Chemical Science and Engineering, School of Materials and Chemical Technology, Institute of Science Tokyo, Tokyo 152-8550, Japan;* orcid.org/0000-0002-3105-4592; Email: satoh@mct.isct.ac.jp

Keiji Tanaka − *Department of Applied Chemistry, Kyushu University, Fukuoka 819-0395, Japan; Center for Polymer Interface and Molecular Adhesion Science, Kyushu University, Fukuoka 819-0395, Japan;* orcid.org/0000-0003-0314-3843; Email: k-tanaka@cstf.kyushu-u.ac.jp

Authors

Shuji Morita − *Department of Applied Chemistry, Kyushu University, Fukuoka 819-0395, Japan*

Shiho Tanizaki − *Department of Chemical Science and Engineering, School of Materials and Chemical Technology, Institute of Science Tokyo, Tokyo 152-8550, Japan*

Tomohiro Kubo − *Department of Chemical Science and Engineering, School of Materials and Chemical Technology, Institute of Science Tokyo, Tokyo 152-8550, Japan;* orcid.org/0000-0003-3913-5845

Satoru Yamamoto − *Center for Polymer Interface and Molecular Adhesion Science, Kyushu University, Fukuoka 819-0395, Japan;* orcid.org/0000-0002-0238-3039

Complete contact information is available at: https://pubs.acs.org/10.1021/jacs.5c23137

Author Contributions

The manuscript was written through contributions of all authors. All authors have given approval to the final version of the manuscript.

Funding

This work was supported by JSPS KAKENHI for Scientific Research (B) (JP23H02014) to K.T. and Scientific Research (C) (JP23K04841) to Y.M. from the Ministry of Education, Culture, Sports, Science, and Technology (MEXT), Japan. We are also thankful for the support from the JST-Mirai Program (JPMJMI18A2) (K.T.) and JST K Program (JPMJKP24W1) (K.T.).

Notes

The authors declare no competing financial interest.

■ ACKNOWLEDGMENTS

We thank Prof. Mark D. Ediger, Prof. Costantino Creton and Prof. Atsushi Takahara for valuable discussions.

■ REFERENCES

(1) Balazs, A. C.; Emrick, T.; Russell, T. P. Nanoparticle Polymer Composites: Where Two Small Worlds Meet. *Science* **2006**, *314*, 1107−1110.

(2) Coates, N. E.; Yee, S. K.; McCulloch, B.; See, K. C.; Majumdar, A.; Segalman, R. A.; Urban, J. J. Effect of Interfacial Properties on Polymer−Nanocrystal Thermoelectric Transport. *Adv. Mater.* **2013**, *25* (25), 1629−1633.

(3) Li, X.; He, S.; Jiang, Y.; Wang, J.; Yu, Y.; Liu, X.; Zhu, F.; Xie, Y.; Li, Y.; Ma, C.; et al. Unraveling Bilayer Interfacial Features and Their Effects in Polar Polymer Nanocomposites. *Nat. Commun.* **2023**, *14*, 5707.

(4) Fielding, J. H. Impact Resilience in Testing Channel Black. *Ind. Eng. Chem.* **1937**, *29*, 880−885.

(5) Fujii, Y.; Yang, Z.; Leach, J.; Atarashi, H.; Tanaka, K.; Tsui, O. K. C. Affinity of Polystyrene Films to Hydrogen-Passivated Silicon and its Relevance to the T_g of the Films. *Macromolecules* **2009**, *42*, 7418−7422.

(6) Jiang, N.; Sen, M.; Endoh, M. K.; Koga, T.; Langhammer, E.; Björn, P.; Tsige, M. Thermal Properties and Segmental Dynamics of Polymer Melt Chains Adsorbed on Solid Surfaces. *Langmuir* **2018**, *34*, 4199−4209.

(7) Krutyeva, M.; Wischnewski, A.; Monkenbusch, M.; Willner, L.; Maiz, J.; Mijangos, C.; Arbe, A.; Colmenero, J.; Radulescu, A.; Holderer, O.; et al. Effect of Nanoconfinement on Polymer Dynamics: Surface Layers and Interphases. *Phys. Rev. Lett.* **2013**, *110*, 1−5.

(8) Adhikari, J. M.; Gadinski, M. R.; Li, Q.; Sun, K. G.; Reyes-Martinez, M. A.; Iagodkine, E.; Briseno, A. L.; Jackson, T. N.; Wang, Q.; Gomez, E. D. Controlling Chain Conformations of High-k Fluoropolymer Dielectrics to Enhance Charge Mobilities in Rubrene Single-Crystal Field-Effect Transistors. *Adv. Mater.* **2016**, *28*, 10095−10102.

(9) Inutsuka, M.; Watanabe, H.; Aoyagi, M.; Yamada, N. L.; Tanaka, C.; Ikehara, T.; Kawaguchi, D.; Yamamoto, S.; Tanaka, K. Effect of Oligomer Segregation on the Aggregation State and Strength at the Polystyrene/Substrate Interface. *ACS Macro Lett.* **2022**, *11*, 504−509.

(10) Van Alsten, J. G.; Sauer, B. B.; Walsh, D. J. Polymer Dynamics at the Melt/Solid Interface: Experimental Evidence of Reduced Center of Mass Mobility. *Macromolecules* **1992**, *25* (25), 4046−4048.

(11) Lin, E. K.; Wu, W. L.; Satija, S. K. Polymer Interdiffusion near an Attractive Solid Substrate. *Macromolecules* **1997**, *30*, 7224−7231.

(12) Popov, I.; Carroll, B.; Bocharova, V.; Genix, A.-C.; Cheng, S.; Khamzin, A.; Kisliuk, A.; Sokolov, A. P. Strong Reduction in Amplitude of the Interfacial Segmental Dynamics in Polymer Nanocomposites. *Macromolecules* **2020**, *53*, 4126−4135.

(13) Li, B.; Chen, L.; Zhang, S.; Tao, Q.; Ma, Y.-H.; Hu, P.; Lu, X.; Chou, K. C.; Chen, Z. Absolute Molecular Structure of the

Polystyrene at the Buried Polystyrene/Silica Interface and its Relationship to Dewetting during Annealing. *Appl. Surf. Sci.* **2023**, *611*, 155715.
(14) Descas, R.; Sommer, J.-U.; Blumen, A. Irreversible Adsorption of Tethered Chains at Substrates: Monte Carlo Study. *J. Chem. Phys.* **2006**, *124*, 094701.
(15) Källrot, N.; Linse, P. Dynamic Study of Single-Chain Adsorption and Desorption. *Macromolecules* **2007**, *40*, 4669−4679.
(16) Bansal, A.; Yang, H.; Li, C.; Cho, K.; Benicewicz, B. C.; Kumar, S. K.; Schadler, L. S. Quantitative Equivalence between Polymer Nanocomposites and Thin Polymer Films. *Nat. Mater.* **2005**, *4*, 693−698.
(17) Rittigstein, P.; Priestley, R. D.; Broadbelt, L. J.; Torkelson, J. M. Model Polymer Nanocomposites Provide an Understanding of Confinement Effects in Real Nanocomposites. *Nat. Mater.* **2007**, *6*, 278−282.
(18) Napolitano, S.; Wübbenhorst, M. The Lifetime of the Deviations from Bulk Behaviour in Polymers Confined at the Nanoscale. *Nat. Commun.* **2011**, *2*, 260.
(19) Tress, M.; Mapesa, E. U.; Kossack, W.; Kipnusu, W. K.; Reiche, M.; Kremer, F. Glassy Dynamics in Condensed Isolated Polymer Chains. *Science* **2013**, *341*, 1371−1374.
(20) Johnson, H. E.; Granick, S. New Mechanism of Nonequilibrium Polymer Adsorption. *Science* **1992**, *255* (255), 966−968.
(21) de Gennes, P. G. Polymers at an Interface; A Simplified View. *Adv. Colloid Interface Sci.* **1987**, *27*, 189−209.
(22) O'Shaughnessy, B.; Vavylonis, D. Irreversibility and Polymer Adsorption. *Phys. Rev. Lett.* **2003**, *90*, 056103.
(23) Merling, W. L.; Mileski, J. B.; Douglas, J. F.; Simmons, D. S. The Glass Transition of a Single Macromolecule. *Macromolecules* **2016**, *49*, 7597−7604.
(24) Riggleman, R. A.; Toepperwein, G.; Papakonstantopoulos, G. J.; Barrat, J.-L.; de Pablo, J. J. Entanglement Network in Nanoparticle Reinforced Polymers. *J. Chem. Phys.* **2009**, *130*, 244903.
(25) Morimitsu, Y.; Matsuno, H.; Oda, Y.; Yamamoto, S.; Tanaka, K. Direct Visualization of Cooperative Adsorption of a String-Like Molecule onto a Solid. *Sci. Adv.* **2022**, *8*, No. eabn6349.
(26) Zhou, Y.; Zhang, J.; Huang, J. Dynamic Propagation Depth in Substrate-Supported Polymer Films: A Molecular Dynamics Simulation. *Macromolecules* **2023**, *56*, 2437−2446.
(27) Kodera, N.; Yamamoto, D.; Ishikawa, R.; Ando, T. Video Imaging of Walking Myosin V by High-Speed Atomic Force Microscopy. *Nature* **2010**, *468*, 72−76.
(28) Kato, H.; Taoka, T.; Nishikata, S.; Sazaki, G.; Yamada, T.; Czajka, R.; Wawro, A.; Nakajima, K.; Kasuya, A.; Suto, S. Preparation of an Ultraclean and Atomically Controlled Hydrogen-Terminated Si(111)-(1 × 1) Surface Revealed by High Resolution Electron Energy Loss Spectroscopy, Atomic Force Microscopy, and Scanning Tunneling Microscopy: Aqueous NH_4F Etching Process of Si(111). *Jpn. J. Appl. Phys.* **2007**, *46*, 5701−5705.
(29) Hao, Z.; Ghanekarade, A.; Zhu, N.; Randazzo, K.; Kawaguchi, D.; Tanaka, K.; Wang, X.; Simmons, D. S.; Priestley, R. D.; Zuo, B. Mobility Gradients Yield Rubbery Surfaces on Top of Polymer Glasses. *Nature* **2021**, *596*, 372−376.
(30) Lee, H.; Dellatore, S. M.; Miller, W. M.; Messersmith, P. B. Mussel-Inspired Surface Chemistry for Multifunctional Coatings. *Science* **2007**, *318*, 426−430.
(31) Banea, M. D.; Rosioara, M.; Carbas, R. J. C.; da Silva, L. F. M. Multi-Material Adhesive Joints for Automotive Industry. *Composites, Part B* **2018**, *151*, 71−77.
(32) García, R.; Paulo, A. S. Attractive and Repulsive Tip-Sample Interaction Regimes in Tapping-Mode Atomic Force Microscopy. *Phys. Rev. B* **1999**, *60*, 4961.
(33) Bradski, G. The OpenCV Library. *Dr. Dobb's J. Softw. Tools* **2000**, *120*, 122−125.
(34) Nečas, D.; Klapetek, P.; Gwyddion. An Open-Source Software for SPM Data Analysis. *Cent. Eur. J. Phys.* **2012**, *10*, 181−188.
(35) Harris, C. R.; Millman, K. J.; van der Walt, S. J.; Gommers, R.; Virtanen, P.; Cournapeau, D.; Wieser, E.; Taylor, J.; Berg, S.; Smith, N. J.; Kern, R.; Picus, M.; Hoyer, S.; van Kerkwijk, M. H.; Brett, M.; Haldane, A.; Del Río, J. F.; Wiebe, M.; Peterson, P.; Gérard-Marchant, P.; Sheppard, K.; Reddy, T.; Weckesser, W.; Abbasi, H.; Gohlke, C.; Oliphant, T. E. Array Programming with NumPy. *Nature* **2020**, *585*, 357−362.
(36) McKenzie, I.; Chai, Y.; Cortie, D. L.; Forrest, J. A.; Fujimoto, D.; Karner, V. L.; Kiefl, R. F.; Levy, C. D. P.; Macfarlane, W. A.; McFadden, R. M. L.; Morris, G. D.; Pearson, M. R.; Zhu, S. Direct Measurements of the Temperature, Depth and Processing Dependence of Phenyl Ring Dynamics in Polystyrene Thin Films by β-detected NMR. *Soft Matter* **2018**, *14*, 7324−7334.
(37) McCrum, N. G.; Read, B. E.; Williams, G. *Anelastic and Dielectric Effects in Polymeric Solids*; Wiley: New York, 1967.
(38) Yano, O.; Wada, Y. Dynamic Mechanical and Dielectric Relaxations of Polystyrene below the Glass Temperature. *J. Polym. Sci., Part A-2* **1971**, *9*, 669−686.
(39) Adam, G.; Gibbs, J. H. On the Temperature Dependence of Cooperative Relaxation Properties in Glass-Forming Liquids. *J. Chem. Phys.* **1965**, *43*, 139−146.
(40) Tanaka, K.; Takahara, A.; Kajiyama, T. Rheological Analysis of Surface Relaxation Process of Monodisperse Polystyrene Films. *Macromolecules* **2000**, *33*, 7588−7759.
(41) Harmandaris, V. A.; Adhikari, N. P.; van der Vegt, N. F. A.; Kremer, K. Hierarchical Modeling of Polystyrene: from Atomistic to Coarse-Grained Simulations. *Macromolecules* **2006**, *39*, 6708−6719.
(42) Tanizaki, S.; Kubo, T.; Bito, Y.; Mori, S.; Aoki, H.; Satoh, K. Development of a Bio-based Adhesive by Polymerization of Boc-Protected Vinyl Catechol Derived from Caffeic Acid. *RSC Sustainability* **2025**, *3*, 1714−1720.
(43) Kaur, S.; Narayanan, A.; Dalvi, S.; Liu, Q.; Joy, A.; Dhinojwala, A. Direct Observation of the Interplay of Catechol Binding and Polymer Hydrophobicity in a Mussel-Inspired Elastomeric Adhesive. *ACS Cent. Sci.* **2018**, *4*, 1420−1429.
(44) Mulama, A. A.; Chandran, S.; Roumpos, K.; Oduor, A. O.; Reiter, G. Dewetting Rheology for Determining Viscoelastic Properties of Nonequilibrated Thin Polymer Films. *Macromolecules* **2019**, *52*, 7894−7903.
(45) Chen, K.; Vyazovkin, S. Isoconversional Kinetics of Glass Aging. *J. Phys. Chem. B* **2009**, *113*, 4631−4635.
(46) Song, Z.; Rodríguez-Tinoco, C.; Mathew, A.; Napolitano, S. Fast Equilibration Mechanisms in Disordered Materials Mediated by Slow Liquid Dynamics. *Sci. Adv.* **2022**, *8*, No. eabm7154.
(47) Kawano, M.; Morimitsu, Y.; Liu, Y.; Miyata, N.; Miyazaki, T.; Aoki, H.; Kawaguchi, D.; Yamamoto, S.; Tanaka, K. In-plane movement of isolated poly(methacrylate) chains on a hydrophilic solid surface. *Macromolecules* **2024**, *57*, 6625−6633.

https://doi.org/10.1021/jacs.5c23137
J. Am. Chem. Soc. XXXX, XXX, XXX−XXX